

1 **Brief communication: Alternation of thaw zones and deep**
2 **permafrost in the cold climate conditions of the East Siberian**
3 **Mountains, Suntar-Khayata Range**

4 Robert Sysolyatin¹, Sergei Serikov¹, Anatoly Kirillin¹, Andrey Litovko¹ and Maxim Sivtsev¹

5 ¹Melnikov Permafrost Institute, Yakutsk, 677000, Russia

6 *Correspondence to:* Robert Sysolyatin (robertseesaw@gmail.com)

7 **Abstract.** The Suntar-Khayata Range include numerous natural phenomena interacting or depending on permafrost
8 conditions. Here, we examine some patterns of deep permafrost and talik zones on adjacent sites. A 210 m deep
9 borehole in siltstone bedrock was equipped in July 2010 for temperature monitoring of the topmost 15 m and
10 measurements of a deep permafrost temperature profile. The temperature curvature in the upper part has a bend which
11 is consistent with at upper portion justify by climate warming and shows a steady-state linear geothermal profile below
12 85 m depth with a high geothermal heat flux. A shallow borehole situated at the river floodplain was used to investigate
13 thaw zones temperature regime. Temperatures down to 6.7 m has been monitored at 5-min intervals during heavy
14 rainfall and has had quite peculiar way. The thickness of the season freezing layer reach to 5.7 m, moreover ground
15 temperature increases to 6 °C at 6.7 m depth by groundwater heat transfer. This study provides some new insight on
16 the permafrost condition at one of the coldest places of Northern Hemisphere.

17 **1 Introductions.**

18 The East Siberian Mountains encompass about half the east Siberia landmass, but at the same time little is known
19 about permafrost of this mountainous terrain. On the other hand, the existing unique environmental conditions and
20 natural cryosphere phenomena (glaciers, aufeis, “Pole of Cold” Oymyakon located at 63°15'N 143°9'E and
21 Verkhoyansk located at 67°33'N 133°23'E e.g.) are interesting for the widespread scientific community (Lytkin and
22 Galanin, 2016; Makarieva et al., 2022; Takahashi et al., 2011). Despite the increasing efforts in global permafrost
23 mapping this area has almost no data on direct permafrost measurements and observations, which would be especially
24 relevant in this data-scarce regions.

25 One of the main permafrost parameter is the permafrost thickness (Osterkamp and Gosink, 1991) which has
26 considerably importance for paleo-climate reconstruction, hydrogeology description, deposit exploitation etc. The
27 permafrost temperatures profile is controlled by initial surface temperature, bedrock thermal properties and
28 geothermal heat flux (Lachenbruch and Marshall, 1986). Most frequently, the data about deep permafrost is acquired
29 during geological-prospecting works for potential deposits. The expensive costs of deep borehole drilling limit its
30 acquisition facilities, but in our case, we have access to a deep open borehole on gold ore deposit. In a previous study
31 we focused on monitoring the active layer temperature regime by a widespread soil-pit network in an area close-by,
32 but the temperature regime at the layer of zero annual amplitude (ZAA), season freezing layer as well as deep
33 temperatures profiles have never been presented before (Sysolyatin et al., 2020).

34 For continuous permafrost of East Siberia, taliks can only exist under specific conditions because of the severe

35 climate. Since the heat balance of the subarctic is clearly not cold enough to induce talik formation, groundwater
36 processes are more often involved. Taliks formed by thermal waters and open taliks (below large rivers) are well
37 known, but taliks confined to coarse-grained permeable sediments of riverbanks are poorly studied (Makarjieva et al.,
38 2019). Floodplain sediments can accumulate water during the warm period and gradually empty in the winter
39 (Mikhailov, 2015). The occurrence of such taliks forms a favorable environment for the growth thermophilic plants
40 out of their species range – e.g., poplar, willow shrub formation.

41 In this brief communication, we present the thermal regime of typical permafrost and talik sites at the Suntar-Khayata
42 Range. The successful embedding of a shallow borehole allows to examine the active layer temperature evolution in
43 a floodplain talik for the first time. We aim to: 1) describe the typical permafrost conditions by possess data and
44 discuss the present temperature changes 2) infer the possible extent of talik zones, discuss the origin of their formation
45 and show the impact of heavy rainfall to ground temperature regime and slope stability. This study presents the general
46 permafrost conditions and discusses possible ways to improve the permafrost mapping of the East Siberian Mountains.

47 **2 Study area.**

48 The Suntar-Khayata Range is located at the southern boundary of the East Siberian Mountains and serves as a
49 watershed between Aldan and Indigirka River basins (Fig. 1). At altitudes between 2000 m asl and 2959 m asl a glacial
50 area is persisting, representing largest of present glaciation in Siberia – with about 195 glaciers cover 163 km²
51 (Ananicheva et al., 2010). The study area is represented by alpine relief with the height of the peaks from 1550 to
52 2031 m asl. The shallow borehole is located at the valley basin of Vostochnaya Khandyga River at 850 m asl (Fig.
53 1d), and the deep borehole is located in the narrow V-shaped valley Vostochnaya Khandyga tributary at 1100 m asl
54 altitude (Fig. 1c). Late Paleozoic sandstone, siltstone and clay slate are prevalent bedrocks of the mountain rock,
55 whereas the valley sediments consist of coarse-grained alluvium strata (Sokolov et al., 2015). Kurums exist at the foot
56 and middle part of the mountain slopes and has widespread distribution (Lytkin and Galanin, 2016) and boulders can
57 reach up to 3 m in diameter.

58 The climate conditions recorded at a weather station 43 km away from to east of the study site (Vostochnaya,
59 WMO24679), situated at 1288 m asl. The MAAT ranges from -15.3°C to -11.2°C, average precipitation is about 280
60 mm and maximum annual snow thickness vary from the 16 to 60 cm for the 1966-2018 period. Direct air temperature
61 observation around the borehole at the floodplain shown the existence of winter temperature inversion at altitudes
62 between 800 and 1400 m asl (Sysolyatin et al., 2020). The flora is not very diverse. Dwarf Siberian pine is occupying
63 the top part of slopes between 1400 and 1600 m asl and able to accumulate significant snow cover. Siberian larch is
64 growing on gentle and steep slopes, flat surfaces reflecting the most severe permafrost conditions. The poplars have a
65 limited extent, adjacent to the riverbank.

66 According to our soil-pit monitoring network (Sysolyatin et al., 2020), the mean annual ground temperature ranges
67 from -1.1 to -10.6°C at 1 m depth, active layer vary from 0.5 to 2.7 m and mean-January ground surface temperature
68 can drop to -31°C. No direct observation of precipitation or snow thickness are available for the study area, but its
69 influence is obviously significant. For instance, in 2021 anomalous heavy rains gave rise to numerous debris flows
70 and the appearance of debris avalanches as well as an abrupt change in the talik temperature regime (Supplementary
71 material, Fig. 3).

72 **3 Materials and method**

73 The deep borehole was drilled for prospecting of the orogenic gold deposit prospecting by a geological company in
74 1991. Organic material is almost absent and soil thickness does not exceed 0.5-0.8 m. Core samples (with marked
75 depths interval) were stocked close to the drilling site, where 4 samples have been collected for laboratory studies. In
76 2010 the sintered ice plug in the topmost 5 m was redrilled for establishing a temperature monitoring site. In 2020,
77 temperature measurements were made at intervals of 5 m for depths of 20 to 150 m and 10 m for depths between 150
78 and 210 m using a movable high-precision negative temperature coefficient thermistor and multiconductor cable. To
79 reduce the impact of convection, the hole was plugged by dense material.

80 The shallow borehole was drilled using a wheeled hammer drilling rig with air circulation in gravel alluvium
81 sediments. Temperature disturbance was assumed to be negligible after a few days. The hole was cased with a PVC
82 pipe with inner diameter of 20 mm and the sensors were inserted at 1, 3, 5 and 6.7 m depths. The space around the
83 casing was filled by sand and well cutting. The first attempt to drill a borehole in the floodplain was reaching to a
84 depth of 12 m, but a failure of drilling tools halted the process. At end of July the stratum was relatively dry.

85 Ground temperatures were monitored continuously within the shallow and deep borehole down to 6.7 and 15 m for
86 one and 9 years, respectively. Measurements were made every 4 h with TMC50-HD thermistors that were attached to
87 four-channel Onset HOBO data loggers (U12-008 model). Air and ground surface temperatures (2 cm depth) were
88 acquired for the shallow borehole site using a 2-channel data logger (U23-003). The operation design of the different
89 logger systems situated at sites and in interior of the boreholes is shown in Table 1. Since the sensors installed in the
90 deep borehole at 5 and 15 m, we report the mean annual ground temperature determine the offset of heat wave
91 penetration from surface. In accordance with local climatic conditions and thermal properties of the bedrock, to
92 account for an equal seasonal cycle, MAGT was calculated for the periods September-August and January-December
93 for depths of 5 and 15 m, respectively. For the shallow boreholes, the data presented for the high-frequency logging
94 period (every 5 min) from 31 July to 8 September are used trace the impact of heavy rain infiltration events on the
95 subsurface thermal regime.

96 **4 Result**

97 *4.1 Permafrost temperature evolution*

98 At the V-valley site, only two of four sensors (5 and 15 m) have useful and reliable data for analysis (Fig 2a and b).
99 The ground temperatures below 0°C were recorded for the whole monitoring period at 5 m depth. The observed
100 average MAGT is -4.25 °C for both depths. The ground temperature evolution shows a sinusoidal pattern with smooth
101 drifting following the changing climate condition. At 5- and 15 m depth, the amplitude ranges from 6.2 to 0.6 °C,
102 respectively, for the whole measurement period. The fluctuations of mean annual ground temperature did not exceed
103 0.61 °C at 5 m and 0.26 °C at 15 m. The warming trend that has been highlighted for the 2010 to 2015 period was
104 changing to equivalent cooling until 2019 at both depths. In accordance with the results presented, the ZAA depth
105 might vary from 10.9 to 13.9 for a thermal diffusivity of around $1.21\text{-}1.96 \times 10^{-6} \text{ m}^2 \text{ s}^{-1}$ by core samples. However, as
106 far as the temperature altering should not up over to 0.1 °C by annual period, the ZAA layer has been exceed 15 m
107 depth.

108 *4.2 Permafrost thickness and thermal conditions*

109 The permafrost thickness observed by these direct measurements does not exceed 205-210 m in the deep borehole at
110 V-valley. A detailed temperature profile is presented in Fig. 2c. Below the assumed depth of ZAA (20 m), the
111 permafrost temperature increases downwards with a gradient ranging from 0.01 to 0.038 °C⁻ m. From the whole

112 temperature curve the mean gradient was calculated as 0.0214 °C m⁻¹. The initial surface temperature ($T_0 = -5.25$ °C) is
 113 obtained by best-fit linear extrapolation from a depth interval of 85-160 m due to the uniform value of the gradient
 114 (Lachenbruch and Marshall, 1986). The values for the temperature anomaly (offset value from linear fit) at 20 m (A_{20})
 115 and 40 m (A_{40}), were calculated as 0.70 and 0.39 °C, respectively.

116 4.3 Talik temperature regime

117 A simple geomorphology sketch of the shallow borehole site is present in Figure 3a and an annual and monthly
 118 temperature-time series for the floodplain site are shown in Figure 3b and c, respectively. The pattern of the 1 m depth
 119 temperature evolution is consistent with the air and surface temperature evolution. Temperatures ranged from -6.3 to
 120 6.6 °C and from -13.7 to 20.7 °C, respectively. Surprisingly, the temperature variation at 3m depth has been smaller
 121 than for the sensors below, just from -2 to 1.6 °C. Refreezing at 3 m depth began at the end of January and the zero-
 122 curtain period is present from approximately the end of June to September, dividing the floodplain (overburden)
 123 sediments into to 3 zones – upper active layer, intermediate frozen layer and bottom permanent talik. The spike in
 124 Figure 3c is related to percolation of warm rainwater to 3 m depth, probably through casing tube. The most peculiar
 125 temperature behavior is found for the 5 and 6.7 m depth sensors, which is surely related to heat advection of ground
 126 water movement. Patterns of temperature changes at 5 m depth are more linear, whereas at 6.7 m it is more exponential.
 127 The maximum absolute temperature ranged between 4.4 °C (5 m) and 7.7 °C (6.7 m), while minimum temperatures
 128 oscillated between -0.2 °C (5 m) and 0.3 °C (6.7 m). The ground at a depth of 5 m remained unfrozen for more than
 129 75% of the time of the year. In an isopleth plot the talik appears below to 5.7 m and obviously continuous downward
 130 (Fig 3b). At an air temperature of -9.9 °C and MAGST of -1.8 °C the MAGT for the observation period (almost a
 131 year) is -1.1, -0.1, 1.1, 1.8 °C for depths of 1, 3, 5 and 6.7 m, respectively.

132 5 Discussion

133 Permafrost thickness is one of the major components of the cryosphere and has a close relation to geothermal heat
 134 flux. According to Balobaev et al. (1985) the Suntar-Khayat Range is characterised by high values of geothermal heat
 135 flux up to 0.08-0.10 Wm⁻² usually concentrating under narrow V-shaped valleys. Through numerous geothermal
 136 measurements at the next orogenic gold deposits (Nezhdaninskoye) specific patterns of thermal conditions were
 137 determined. Thus, the angle of inclination of the surface reduces the geothermal heat flux according to the equation:

$$138 \quad q = q_0 \cos \alpha \quad (1)$$

139 where q – calculated geothermal heat flux; q_0 – initial geothermal heat flux, α – slope angle.

140 The interaction between altitude and surface temperature has also been presented in previous studies and might
 141 decrease MAGST to -6.5°C at 1800 m asl mountain peaks (Sysolyatin et al., 2020). As mentioned above, MAGT at 5
 142 m depth have rather similar value to the ZAA temperature. By the steady-state equation (2) and expect the decrease
 143 of the ZAA temperature upon upward height, the permafrost thickness was calculated (Table 1) (Carslow and Jager,
 144 1959; Guglielmin et al., 2011). By core samples, bedrock effective thermal conductivity is 2.41 Wm⁻¹ K⁻¹ and $q_0 =$
 145 0.052 Wm⁻² in permafrost body at base altitude surface level – 1100 m According to the orographic configuration of
 146 the study area, the permafrost thickness at local peaks 2000 m asl can reach to ~ 500 m.

$$147 \quad Z = T * \frac{\lambda}{q} + ZAA \quad (2)$$

148 where, Z – estimated permafrost thickness, m; T – temperature at the ZAA depth, °C; λ – effective thermal
149 conductivity, $\text{Wm}^{-1} \text{ } ^\circ\text{C}^{-1}$; q – geothermal heat flux in permafrost Wm^{-2} (from equation 1).

150 Extrapolation of the linear portion of temperature curve to the surface result in significant differences to the current
151 temperature curve from the initial MAGST features (Lachenbruch and Marshall, 1986). Two variants of changes are
152 considered, a temperature change at the surface and a temperature change at the ZAA. For instance, assuming thermal
153 diffusivity is $1.6 \times 10^{-6} \text{ m}^2 \text{ s}^{-1}$, the surface temperature shift around $1.4 \text{ } ^\circ\text{C}$ would be ongoing from 22 to 81-year respect
154 to step, linear or exponential way of changes. When the temperature shifts by $0.7 \text{ } ^\circ\text{C}$ at the ZAA, the response time
155 will expand to a range of 19 to 90 years. With the available data about the rate of air temperature change at the closest
156 weather station, the second variant is the most plausible. It should be noted that the snow cover can change the surface
157 temperature by more than $5 \text{ } ^\circ\text{C}$ (Gisnas et al., 2014), which is much larger than the air temperature change over the
158 last 80 years (IPCC, 2014).

159 As mentioned above, the talik appearance can only be caused by the thermal influence of superficial or ground water
160 in the cold environments of northeastern Siberia. The absence of permafrost under large rivers and in the areas adjacent
161 to hot springs is well-known. Nevertheless, in our case, where the distance from the main stream exceeds 1 km, the
162 presence of the talik was not assumed before. The reason for the existence of the talik is ambiguous. One possibility
163 is the migration of rainwater infiltrating through the "windows" of the kurums (block streams) on the adjacent slope.
164 The timing of the thermal impact of rainfall is clearly evident on the temperature graph at a depth of 1 m. These spikes
165 have been well explained before (Hinkel et al., 2001). The divergent temperature response at depths of 5 and 6.7 m is
166 difficult to explain, perhaps it may be related to the interaction of rainfall with the permafrost occurrence at depth. It
167 could also have been due to a delay in the influence of groundwater supply from the river. However, the response time
168 is largely consistent with the first hypothesis. The influence of groundwater from the river when considering the
169 thawing cycle is certain. On the isopleth plot it is clearly shown that the temperature at the depth of 5 and 6.7 m begins
170 to increase earlier than at a depth of 3 m, which means the proximity to the groundwater is accelerating warming for
171 the coarse-grained sediments. To solve this issue, it would be necessary to install additional piezometric and
172 temperature monitoring sites, as well as to carry out temperature measurements of the river water.

173 The interactions between groundwater and permafrost have been examined in a numerous study (e.g. Ge et al., 2011;
174 Kane et al., 2013; Walvoord and Kurylyk, 2016). But the features of floodplain taliks for Kolyma region are considered
175 rather recently and are not well understood (Mikhailov, 2015). It is noted as the crucial reason for the formation of the
176 winter river flow. Floodplain taliks of the region are capable to accumulate huge amounts of water and gradually
177 return it back to the river during low-flow cold season. The main influencing factors are the slope of the river
178 floodplain and the permeability of the sediments. The volume of the sand backfill material usually decreases
179 downward to the aquiclude which increases permeability and capaciousness of the aquifer. Probably the reason for
180 the appearance of such a large talik is just related to the site-specific conditions of the study area. A sufficiently reliable
181 marker may be the areal of poplar trees, tending to warmer environments. However, in our case, at the drilling site the
182 vegetation was represented by mosses and larch that is more typical for permafrost landscapes.

183 An increase in liquid precipitation, along with increase in air temperature, is one of the most obvious consequences
184 of global warming (Savelieva et al., 2000; Yang et al., 2005). For the permafrost zone, heavy rainfall often acts as a
185 trigger for geomorphological processes (Borgatti and Soldati, 2013). The effect of heavy rainfalls on permafrost is
186 most pronounced for the mountainous areas.

187 The behavior of the upper part of the permafrost during flooding rains, creates reasons for the activation of slope
188 processes. Heavy rains at the end of August 2021 were the trigger for 7 large landslides on a 5 km section of the
189 Kolyma highway, temporarily stopping traffic (Supplementary material). The high concentration of landslides on this
190 section is explained by the aspect and angle of the slope, creating favorable conditions for an increase of the active
191 layer. Abrupt and abundant saturation with rainwater led to critical weighting of soil material, after which the stability
192 of the slope has been disrupted. Landslide processes were also observed everywhere during field investigations in
193 other areas with a lower inclination and northern and eastern aspects. Descriptions of such scenarios are given in many
194 sources, but the detailed process for regions of northeastern Siberia is poorly understood at this time (Frauenfelder et
195 al., 2018; Geertsema et al., 2006; Gruber and Haeberli, 2007).

196 **6 Conclusion**

197 This study provides insight into thermal patterns of permafrost and talik that can be valuable for future studies of the
198 East Siberian Mountains. Permafrost is almost continuously distributed with a thickness reach to 500 m. Thermal
199 properties of the bedrock were obtained through laboratory determinations and a negligible permafrost temperature
200 trend was identified as a result of long-term monitoring. Due to the successful location of the borehole and high-
201 frequency measurements during rare heavy rains in August 2021, unusually high values of daily precipitation were
202 recorded in the Suntar Khayata Mountains (Verkhoyansk Ridge, Siberia). Due to the abundance of liquid precipitation,
203 peculiarities of the configuration of permafrost and thaw zones, as well as site morphology, the temperature regime
204 of soils has a peculiar feature down to a depth of 6.7 m. The size of the talik zone can be very significant, which must
205 be considered in mapping, design and modeling. A wide range of multidisciplinary research is required to improve
206 the understanding of permafrost conditions in this area.

207 *Data availability*

208 The data are available from the authors upon request.

209 *Supplement*

210 Debris landslides evidence are added at Supplement material.

211 *Author contributions*

212 RG and SS proposed the initial idea and carried out this study by designing researching sites, analyzing data, and
213 organizing and was responsible for the compilation and quality control of the observations. RG, SS, AL and MS
214 handled with field works. AK responsible for laboratory determination of rock thermal properties. RG prepared the
215 manuscript with contributions from SS, AK, AL and MS.

216 *Competing interests*

217 The authors declare that they have no conflict of interest.

218 **Acknowledgments**

219 This study has been funded by Republic of Sakha (Yakutia) and Russian Science Foundation (project N 22-27-20073).
220 The authors acknowledge the Melnikov Permafrost Institute for logistic and field work support. Finally, we thank the
221 reviewer Lutz Schirrmeister, anonymous reviewer, and editor Christian Hauck for comments, suggestions and
222 technical corrections which helped improve the manuscript.

223 **References**

- 224 Ananicheva, M. D., Krenke, A. N. and Barry, R. G.: The Northeast Asia mountain glaciers in the near future by
225 AOGCM scenarios, *Cryosph.*, 4(4), 435–445, doi:10.5194/tc-4-435-2010, 2010.
- 226 Balobaev, V. T., Devyatkin, V. N., Gavriliev, R. I. and Rusakov, V. G.: About geothermophysical researching of
227 mineral deposits at north-east region, *Geol. Geol. Explor.*, 5, 36–37, 1985.
- 228 Borgatti, L. and Soldati, M.: 7.30 Hillslope Processes and Climate Change, in *Treatise on Geomorphology*, pp. 306–
229 319, Elsevier., 2013.
- 230 Carslow, H. S. and Jager, J. C.: *Conduction of Heat in Solids*, Oxford University Press: New York., 1959.
- 231 Frauenfelder, R., Isaksen, K., Lato, M. J. and Noetzli, J.: Ground thermal and geomechanical conditions in a
232 permafrost-affected high-latitude rock avalanche site (Polvartinden, northern Norway), *Cryosph.*, 12(4), 1531–1550,
233 doi:10.5194/tc-12-1531-2018, 2018.
- 234 Ge, S., McKenzie, J., Voss, C. and Wu, Q.: Exchange of groundwater and surface-water mediated by permafrost
235 response to seasonal and long term air temperature variation, *Geophys. Res. Lett.*, 38(14), L14402,
236 doi:10.1029/2011GL047911, 2011.
- 237 Geertsema, M., Clague, J. J., Schwab, J. W. and Evans, S. G.: An overview of recent large catastrophic landslides in
238 northern British Columbia, Canada, *Eng. Geol.*, 83(1–3), 120–143, doi:10.1016/j.enggeo.2005.06.028, 2006.
- 239 Gisnas, K., Westermann, S., Schuler, T. V., Litherland, T., Isaksen, K., Boike, J. and Etzelmuller, B.: A statistical
240 approach to represent small-scale variability of permafrost temperatures due to snow cover, *Cryosphere*, 8(6), 2063–
241 2074, doi:10.5194/tc-8-2063-2014, 2014.
- 242 Gruber, S. and Haerberli, W.: Permafrost in steep bedrock slopes and its temperature-related destabilization
243 following climate change, *J. Geophys. Res. Surf.*, 112(F2), doi:10.1029/2006jf000547, 2007.
- 244 Guglielmin, M., Balks, M. R., Adlam, L. S. and Baio, F.: Permafrost Thermal Regime from Two 30-m Deep
245 Boreholes in Southern Victoria Land, Antarctica, *Permafr. Periglac. Process.*, 22(2), 129–139, doi:10.1002/ppp.715,
246 2011.
- 247 Hinkel, K. M., Paetzold, F., Nelson, F. E. and Bockheim, J. G.: Patterns of soil temperature and moisture in the
248 active layer and upper permafrost at Barrow, Alaska: 1993–1999, *Glob. Planet. Change*, 29(3–4), 293–309,
249 doi:10.1016/S0921-8181(01)00096-0, 2001.
- 250 IPCC: *Climate Change 2014*, in *Synthesis Report, Contribution of Working Groups I, II and III to the Fifth*
251 *Assessment Report of the Intergovernmental Panel on Climate Change*, p. 151, Geneva, Switzerland., 2014.
- 252 Kane, D. L., Yoshikawa, K. and McNamara, J. P.: Regional groundwater flow in an area mapped as continuous
253 permafrost, NE Alaska (USA), *Hydrogeol. J.*, 21(1), 41–52, doi:10.1007/s10040-012-0937-0, 2013.
- 254 Lachenbruch, A. H. and Marshall, B. V.: Changing Climate: Geothermal Evidence from Permafrost in the Alaskan
255 Arctic, *Science (80-.)*, 234(4777), 689–696, doi:10.1126/science.234.4777.689, 1986.
- 256 Lytkin, V. M. and Galanin, A. A.: Rock glaciers in the Suntar-Khayata Range, *Ice Snow*, 56(4), 511–524,
257 doi:10.15356/2076-6734-2016-4-511-524, 2016.

258 Makarieva, O., Nesterova, N., Post, D. A., Sherstyukov, A. and Lebedeva, L.: Warming temperatures are impacting
259 the hydrometeorological regime of Russian rivers in the zone of continuous permafrost, *Cryosph.*, 13(6), 1635–
260 1659, doi:10.5194/tc-13-1635-2019, 2019.

261 Makarieva, O., Nesterova, N., Shikhov, A., Zemlianskova, A., Luo, D., Ostashov, A. and Alexeev, V.: Giant
262 Aufeis—Unknown Glaciation in North-Eastern Eurasia According to Landsat Images 2013–2019, *Remote Sens.*,
263 14(17), 4248, doi:10.3390/rs14174248, 2022.

264 Mikhailov, V. M.: Geographical regularities of distribution of floodplain taliks, *Izv. Ross. Akad. Nauk. Seriya*
265 *Geogr.*, (1), 65, doi:10.15356/0373-2444-2014-1-65-74, 2015.

266 Osterkamp, T. E. and Gosink, J. P.: Variations in permafrost thickness in response to changes in paleoclimate, *J.*
267 *Geophys. Res. Solid Earth*, 96(B3), 4423–4434, doi:10.1029/90JB02492, 1991.

268 Savelieva, N. ., Semiletov, I. ., Vasilevskaya, L. . and Pugach, S. .: A climate shift in seasonal values of
269 meteorological and hydrological parameters for Northeastern Asia, *Prog. Oceanogr.*, 47(2–4), 279–297,
270 doi:10.1016/S0079-6611(00)00039-2, 2000.

271 Sokolov, S. D., Tuchkova, M. I., Ganelin, A. V., Bondarenko, G. E. and Layer, P.: Tectonics of the South Anyui
272 Suture, Northeastern Asia, *Geotectonics*, 49(1), 3–26, doi:10.1134/S0016852115010057, 2015.

273 Sysolyatin, R., Serikov, S., Zheleznyak, M., Tikhonravova, Y., Skachkov, Y., Zhizhin, V. and Rojina, M.:
274 Temperature monitoring from 2012 to 2019 in central part of Suntar-Khayat Ridge, Russia, *J. Mt. Sci.*, 17(10),
275 2321–2338, doi:10.1007/s11629-020-6175-3, 2020.

276 Takahashi, S., Sugiura, K., Kameda, T., Enomoto, H., Kononov, Y., Ananicheva, M. D. and Kapustin, G.: Response
277 of glaciers in the Suntar–Khayata range, eastern Siberia, to climate change, *Ann. Glaciol.*, 52(58), 185–192,
278 doi:10.3189/172756411797252086, 2011.

279 Walvoord, M. A. and Kurylyk, B. L.: Hydrologic Impacts of Thawing Permafrost-A Review, *Vadose Zo. J.*, 15(6),
280 vzt2016.01.0010, doi:10.2136/vzt2016.01.0010, 2016.

281 Yang, D., Kane, D., Zhang, Z., Legates, D. and Goodison, B.: Bias corrections of long-term (1973-2004) daily
282 precipitation data over the northern regions, *Geophys. Res. Lett.*, 32(19), n/a-n/a, doi:10.1029/2005GL024057,
283 2005.

284

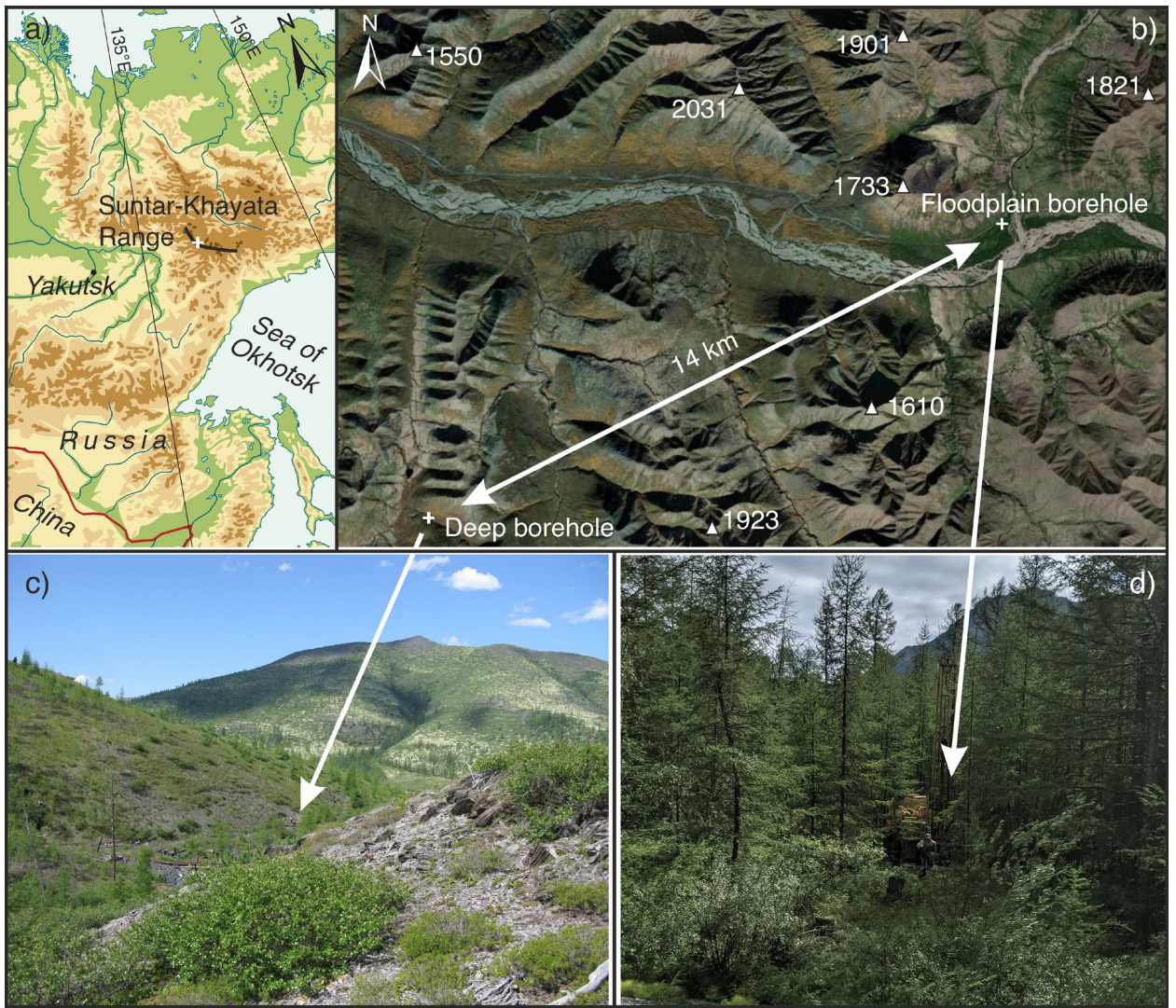
285

286

287

288

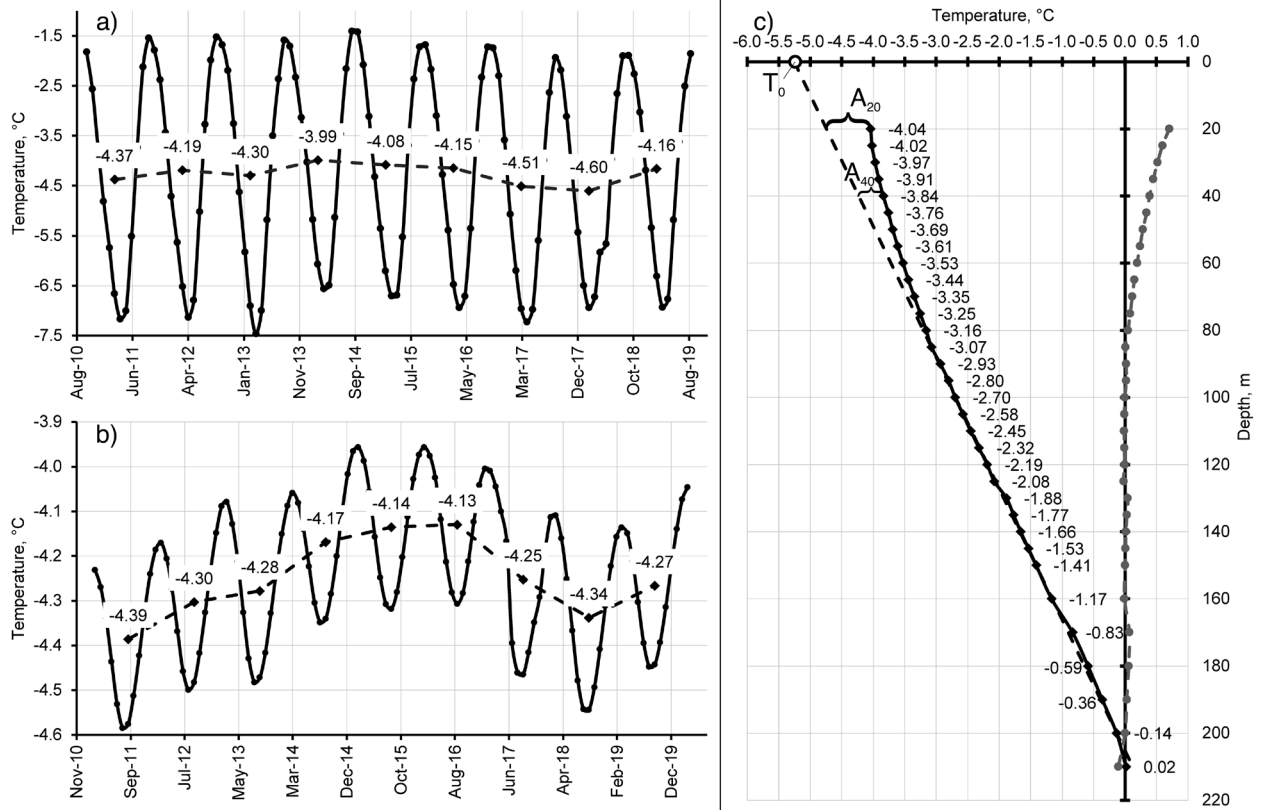
289



290

291 **Figure 1. Study area description and picture of sites environment. In (a) a modified physical map of the location of the study**
 292 **area in eastern Siberia is shown (Map source: © GEOATLAS 1998). (b) MAXAR image of Vostochnaya Khandyga basin**
 293 **with altitudes of peaks. (c) Deep borehole site at V-shaping valley. (d) Shallow borehole site at river plain.**

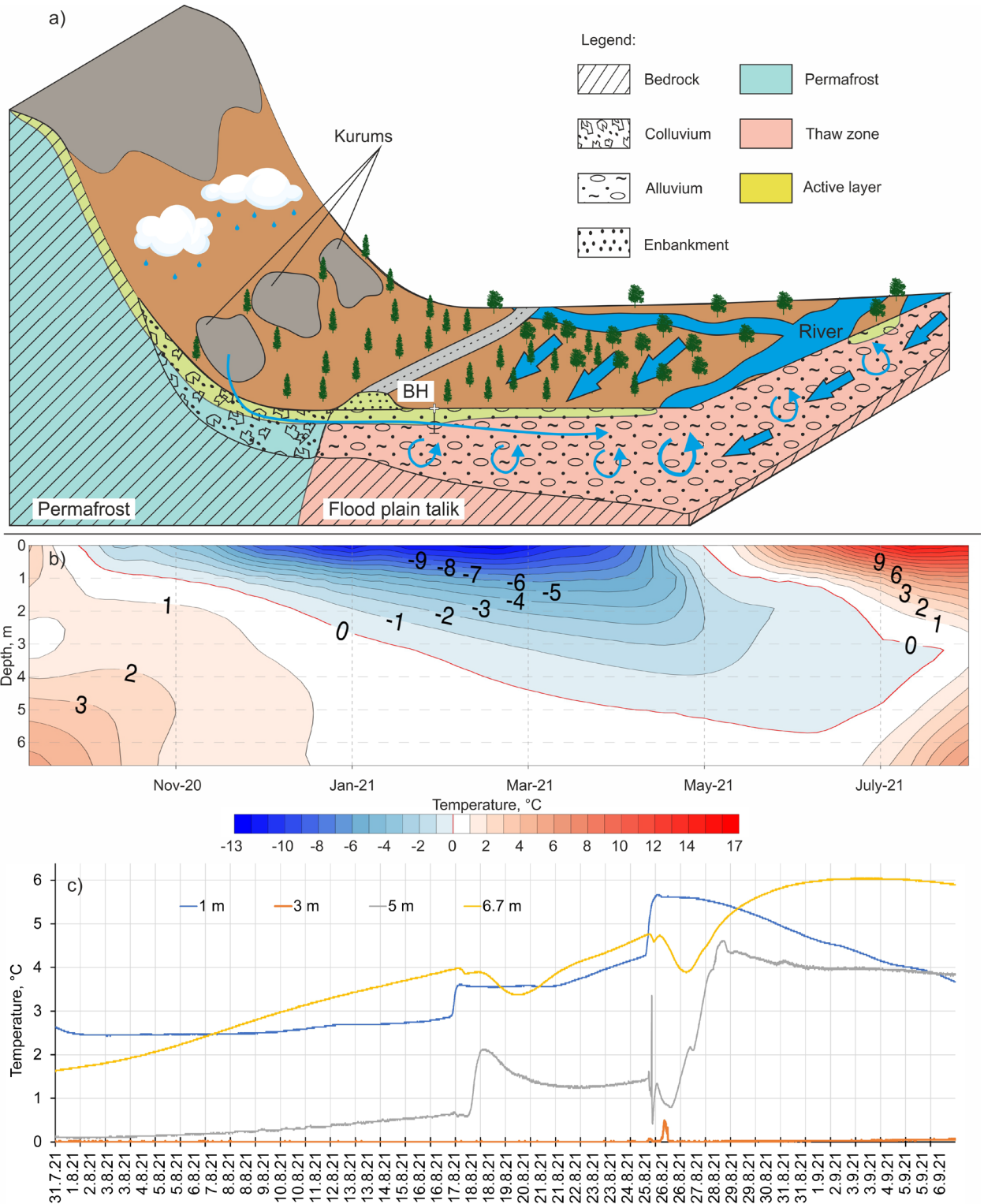
294



295

296 **Figure 2: Thermal regime of permafrost conditions in the deep borehole. Mean monthly and annual ground temperature**
 297 **evolution at 5 m (a) and 15 m (b) depth. (c) Temperature profile (solid line), best linear-fit (dashed line) and current offset**
 298 **from extrapolated temperature (dotted line).**

299



300

301 **Figure 3: (a) The scenario of ground water flow of the floodplain talik. (b) Annual ground temperature evolution and (c)**
 302 **temperature fluctuation at a heavy rain event.**

303

304

305

306

307

Table 1

308 General parameters of equipment and operating timing of the loggers installed at different depths inside the
 309 boreholes during the control period.

Location	Logger system and sensor	Accuracy and operation range	Sensor's depth, m	Measuring interval and operating time
River flood plain, Shallow borehole	OnSet Hobo U12-008	± 0.25 °C at range -40 to 100 °C	1, 3, 5, 6.7	Every 5 min from 31-Jul-2021 to 7-Sep-2021/ Every 4 h from 8-Sep-2021 to 18-Aug-2022
River flood plain, Shallow borehole	OnSet Hobo U23-003		Air, Surface	
V-shaped valley, Deep borehole	OnSet Hobo U12-008		1*, 5, 10**, 15	Every 4 h from 20-Jul-2010 to 9-Sep-2021

310 *non valid cause to close position to borehole's iron case tube

311 **non valid because of misgiving temperature data at long period

312

313

Table 2

314 Permafrost thickness based on the assumption that MAGT and permafrost heat flow are decreasing under step-up of
 315 peaks height.

Peak altitude, m	Slope inclination (α), grad	Cos α	Temperature at ZAA (20 m depth), °C	q, Wm ⁻² ,	Permafrost thickness, m
1550	24.2	0.912	-5.5	0.047	298
1600	26.6	0.894	-5.7	0.047	314
1700	31.0	0.857	-6.0	0.045	343
1800	35.0	0.819	-6.5	0.043	386
1900	38.7	0.781	-7.0	0.041	434
2000	42.0	0.743	-7.5	0.039	486

316